

Review

Carbon Cycling in the World's Mangrove Ecosystems Revisited: Significance of Non-Steady State Diagenesis and Subsurface Linkages between the Forest Floor and the Coastal Ocean

Daniel M. Alongi 

Tropical Coastal & Mangrove Consultants, 52 Shearwater Drive, Pakenham, VIC 3810, Australia; dmalongi@outlook.com; Tel.: +61-471448687

Received: 6 August 2020; Accepted: 7 September 2020; Published: 10 September 2020



Abstract: Carbon cycling within the deep mangrove forest floor is unique compared to other marine ecosystems with organic carbon input, mineralization, burial, and advective and groundwater export pathways being in non-steady-state, often oscillating in synchrony with tides, plant uptake, and release/uptake via roots and other edaphic factors in a highly dynamic and harsh environment. Rates of soil organic carbon (C_{ORG}) mineralization and belowground C_{ORG} stocks are high, with rapid diagenesis throughout the deep (>1 m) soil horizon. Pocketed with cracks, fissures, extensive roots, burrows, tubes, and drainage channels through which tidal waters percolate and drain, the forest floor sustains non-steady-state diagenesis of the soil C_{ORG} , in which decomposition processes at the soil surface are distinct from those in deeper soils. Aerobic respiration occurs within the upper 2 mm of the soil surface and within biogenic structures. On average, carbon respiration across the surface soil-air/water interface ($104 \text{ mmol C m}^{-2} \text{ d}^{-1}$) equates to only 25% of the total carbon mineralized within the entire soil horizon, as nearly all respired carbon ($569 \text{ mmol C m}^{-2} \text{ d}^{-1}$) is released in a dissolved form via advective porewater exchange and/or lateral transport and subsurface tidal pumping to adjacent tidal waters. A carbon budget for the world's mangrove ecosystems indicates that subsurface respiration is the second-largest respiratory flux after canopy respiration. Dissolved carbon release is sufficient to oversaturate water-column $p\text{CO}_2$, causing tropical coastal waters to be a source of CO_2 to the atmosphere. Mangrove dissolved inorganic carbon (DIC) discharge contributes nearly 60% of DIC and 27% of dissolved organic carbon (DOC) discharge from the world's low latitude rivers to the tropical coastal ocean. Mangroves inhabit only 0.3% of the global coastal ocean area but contribute 55% of air-sea exchange, 14% of C_{ORG} burial, 28% of DIC export, and 13% of DOC + particulate organic matter (POC) export from the world's coastal wetlands and estuaries to the atmosphere and global coastal ocean.

Keywords: biogeochemistry; carbon; carbon cycling; coastal ocean; export; non-steady-state; mangrove; mangrove carbon budget; moil; subsurface transport

1. Introduction

Mangrove forests have the largest organic carbon (C_{ORG}) stocks of any tropical terrestrial or marine ecosystem [1,2], with a global mean total forest stock of 738.9 ± 27.9 (± 1 standard error, SE) $\text{Mg } C_{ORG} \text{ ha}^{-1}$, of which 76.5% is stored in the soil, 14.8% vested in aboveground biomass and the remaining 8.7% vested in belowground roots [3]. These large amounts of organic carbon reflect high mangrove primary productivity, equal to those of tropical humid evergreen forests and coral reefs [2] and rapid rates of soil accretion on the forest floor.

Mangroves function like other forested ecosystems in exchanging gases with the atmosphere but are like other coastal tidal wetlands in exchanging gases and dissolved and particulate materials with adjacent coastal waters. Mangrove ecosystems are thus tightly linked to land, ocean, and atmosphere, yet still, store vast quantities of C_{ORG} and other elements in their soils and forest biomass. While mangroves have some features of both terrestrial and coastal ecosystems, they do have a number of unique ecological and physiological characteristics [4] that enable them to efficiently utilize and sequester carbon and nutrient elements, especially nitrogen, phosphorus, iron, and copper [5,6].

The biogeochemical connections between mangroves and adjacent tidal waters are complex, with variable concentrations of dissolved organic and inorganic solutes and particulates imported and exported by both tides, porewater pumping, and subsurface groundwater advection [7]. Tidal circulatory processes, such as a pronounced asymmetry between ebb and flood tides (with the ebb tide being shorter in duration but with stronger current velocity than the flood tide); friction, flow resistance, drag of tidal waters due to the presence of aboveground and belowground structures, lateral trapping (water flowing in and out of a waterway is temporarily retained in the forest to be returned to the main channel later), and lateral gradients due to high evapotranspiration [8]. Interrelated processes exert control over sediment transport and deposition: (1) tidal pumping, (2) baroclinic circulation, (3) particle trapping in the turbidity maximum, (4) flocculation, (5) the mangrove tidal prism, (6) physiochemical reactions that destroy cohesive flocs, and (7) microbial production of mucus. Sedimentation of particles is often rapid in quiescent mangrove environments, resulting in a global mean carbon sequestration rate of $179.6 \pm 16.4 \text{ gC m}^{-2} \text{ a}^{-1}$ [3]. Over decades, after initial colonization of a mudflat, the forest develops and the floor builds up further, adjusting to sea-level, subsidence, and uplift, with the net result being several meters of soil [9]. Over time, these deposits are penetrated further by mangrove trees and their extensive root systems, various other flora (e.g., microalgae) and fauna, especially burrowing crabs, and highly abundant and productive microbial communities [10]. The forest floor is thus ordinarily pockmarked with mounds, burrows, tubes, cracks, fissures, coarse and fine living and dead roots and root hairs, and layered with decayed wood, litter, crawling epifauna, and various forms of micro- and macroalgae. Mangrove deposits contribute about 30% to carbon storage on the coastal margins in subtropical and tropical latitudes [11].

Mangrove ecosystems similarly contribute a disproportionate share of various forms of carbon to the coastal ocean in low latitudes. Although they occupy only 1.5% of the world's subtropical and tropical coastal ocean area, mangroves account for about 5% of net primary production and 12% of ecosystem respiration. How much mangrove particulate carbon (i.e., litter) is exported to adjacent waters is well-known [7,12], but how much mangrove ecosystems contribute to dissolved inorganic carbon (DIC) discharging into low latitude coastal waters is unclear [11], as are the amounts of carbon gases released from mangrove waters to the atmosphere. How much soil carbon is mineralized throughout the entire soil horizon is poorly understood, with the current knowledge based mostly on measurements of oxygen consumption and DIC and CO_2 production at the surface soil-air/water interface. The functional link between these processes within the forest floor and the adjacent coastal zone has remained similarly unquantified until only very recently [13].

This paper critically examines the traditionally measured rates of soil respiration and compares these data with rates of belowground DIC production, highlighting any discrepancies to accurately estimate rates of C_{ORG} mineralization throughout the deep forest floor. This information is then compared with recent estimates of DIC export via subsurface pathways to determine its significance in mangrove carbon cycling and the functional links between the mangrove forest floor and the adjacent coastal ocean. A revised carbon mass balance for the world's mangroves is then presented to identify the major and minor pathways of carbon flow as well as what further empirical measurements are needed to improve our knowledge of carbon balance in these tidal ecosystems

2. Rates of Surface and Subsurface Soil C_{ORG} Mineralization

Microbial decomposition of soil organic matter in mangroves involves several anaerobic diagenetic reactions and transport processes. Once oxygen is depleted in surface soils (upper 2 mm) by aerobic respiration, several groups of anaerobic bacteria decompose soil organic carbon via the reduction of sulfate, iron, and manganese, production of methane (methanogenesis); the production of gaseous nitrogen (denitrification) also occurs but are ordinarily minor carbon decomposition processes [14]. However, the availability of organic carbon molecules for anaerobic microbial breakdown requires prior fermentation to generate low molecular weight organic substrates, such as lactate, butyrate, propionate, and acetate. Which reaction dominates early diagenesis depends on several drivers, such as geomorphologic setting, salinity, frequency of tidal inundation, temperature, the degree of freshwater, marine and terrestrial inputs, root physiological activities, the quantity and quality of organic matter, the intensity of disturbance from benthic organisms (i.e., bioturbation), and accretion rates [14,15] as does forest age, soil C_{ORG} and nutrient content, tree densities, and mangrove species composition.

Soil properties vary widely among mangrove forests, and although these soils are often described as highly reducing and sulfidic, most forest deposits cannot be so simplistically described [15]. Soil texture and associated physicochemical properties depend on the nature of the environment (quiescent or physically dynamic), the distribution of trees and their roots, geomorphology, rainfall, and the source of the organic matter and parent rock. Forests located in large river deltas and in quiescent areas most often possess soils that are predominantly well-sorted silt and clay, with large quantities of fibrous root matter; higher concentrations of sand occur in soils in forests in more active locations, such as swift-flowing rivers. Below a thin veneer of oxidized surface soil, animal burrows, and tube walls, mangrove soils are usually suboxic (no free oxygen but solutes with bound oxygen, e.g., nitrate) and anoxic (no oxygen), but rarely sulfidic (containing HS⁻, H₂S); sulfidic zones occur where roots and other biogenic structures are absent and commonly where there are large surface deposits of litter, especially leaves and clumps of dead roots. In subsurface soils to a depth of 1 m, redox potential (Eh) is usually within the range of -200 to +300 mV [15]. In short, there is no one simplistic definition of what constitutes mangrove soil.

2.1. Respiration at the Soil Surface

Aerobic decomposition of labile C_{ORG} at and near the soil surface usually occurs rapidly, resulting in O₂ rarely penetrating more than 2 mm into the soil. Except for translocation of O₂ into deeper soils via tree roots and crab burrows, most decomposition is suboxic and/or anoxic. Measurements of dissolved and gaseous O₂ consumption across the forest floor surface are common as the methodology is comparatively simple, especially with technological advances in the sensitivity and stability of oxygen probes; gas measurements are somewhat more complex, requiring the need for gas chromatography.

The notion that measurements of O₂ consumption and CO₂ and DIC release at the soil/sediment surface in aquatic sediments reflect carbon mineralization within the entire soil/sediment deposit assumes that (1) the molecular diffusion of these solutes from the sediment/soil surface is constant; (2) in the case of oxygen, most of the O₂ is driven by oxidation of reduced metabolites (e.g., HS⁻, Fe²⁺) diffusing from deeper sediment layers, thus represents total carbon oxidation within the deposit; and (3) these measurements assume steady-state diagenetic conditions, that is, that the rate of molecular diffusion of gases and solutes from soils/sediments to overlying waters or the atmosphere is constant. Non-steady state conditions mean that the rate of diffusion is a function of time (i.e., it changes with time).

Rates of O₂ and dissolved oxygen (DO) consumption and DIC and CO₂ release from mangrove soils (Figure 1) were rapid compared with those from other estuarine and marine benthic environments [10,16]. Rates of O₂ consumption in exposed soils were significantly higher than DO consumption rates from inundated soils (one-way analysis of variance on rank and Dunn's method for multiple comparisons; Dunn's Q = 3.051). Similarly, rates of CO₂ release from exposed soils were higher than rates of DIC release from inundated soils (Dunn's Q = 2.701). Rates of DO and DIC

fluxes across inundated soils were significantly different, with higher DIC fluxes (Dunn's $Q = 2.739$). In contrast, differences in O_2 and CO_2 gas fluxes were not significantly different (Dunn's $Q = 1.891$). The mean respiratory quotient (RQ) for inundated soils was 1.83 ± 0.24 (± 1 SE) and the RQ for exposed soils was 1.73 ± 0.35 . O_2 and CO_2 fluxes from exposed soils were more rapid as gases diffuse more quickly than solutes.

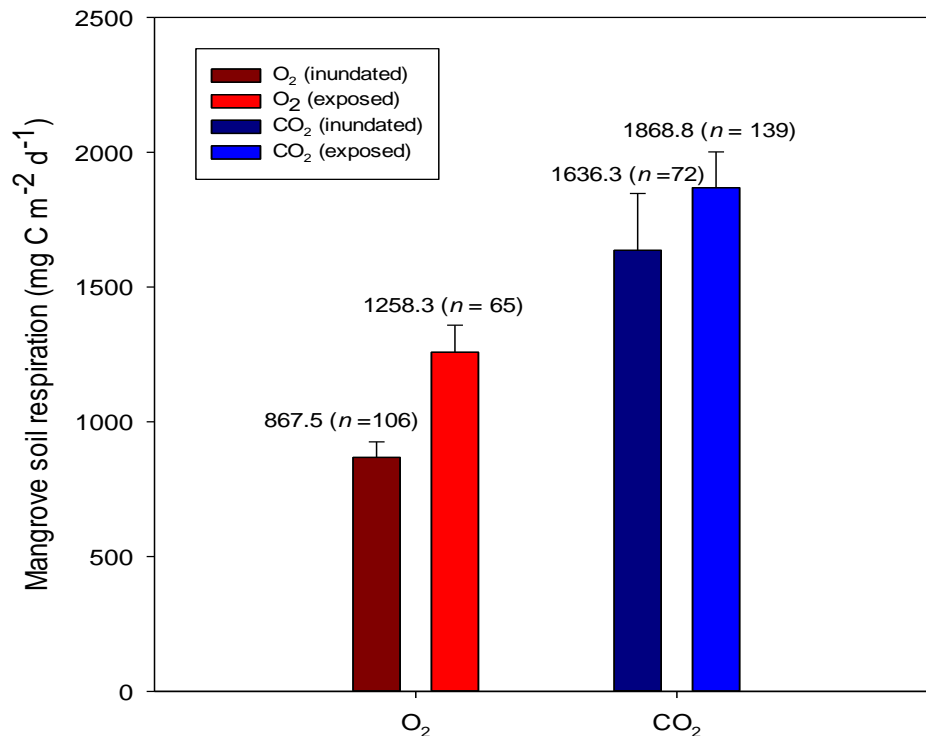


Figure 1. Mean (± 1 standard error) rates of dissolved and gaseous oxygen consumption and dissolved inorganic carbon (DIC) production and CO_2 release ($mg\ C\ m^{-2}\ d^{-1}$) from tidally inundated and exposed mangrove soils, respectively. Field measurement and soil incubation data from references [17–54] were obtained from searches of the Web of Science and Google Scholar.

2.2. Rates of DIC Production within the Forest Floor

The production of respired CO_2 by microbial communities in mangrove soils has been measured using a simple technique of incubating subsamples of soils taken at different depths under oxygen-free conditions and obtaining DIC built up in the incubated samples over several days [53,54]. This method has its drawbacks, such as possible loss of DIC via authigenic mineral formation (i.e., precipitation of carbonates) and lack of linear increase in DIC production over the time course of the experiments. As most of the incubations were conducted using soils from a depth of 10–50 cm or less, all data were extrapolated here to 100 cm by simple multiplication, based on the fact that no DIC production profiles indicate a clear increasing or decreasing trend with soil depth [53–63]. An example of such profiles (Figure 2) from four Australian mangrove sites depicts the typical lack of clear trends with increasing depth, suggesting that extrapolation to 1 m depth is reasonable. The irregular pattern with soil depth is likely the result of several interrelated factors: (1) subsurface microbial decomposition stimulated by root and bioturbation activities; (2) tidal flushing and percolation of rainwater into the forest floor keeps the interstitial water circulating, preventing the buildup of toxic metabolites; (3) while labile organic matter content usually declines with soil depth, there is usually no clear trend in dissolved organic carbon (DOC) and nitrogen concentrations; and (4) mangrove roots typically excrete labile organic metabolites into the soil, likely stimulating microbial activity [15]. From a microbial perspective, the forest floor acts like a sponge, serving as a deep diagenetic reactor that is alternately drained and replenished with oxidized solutes and gases.

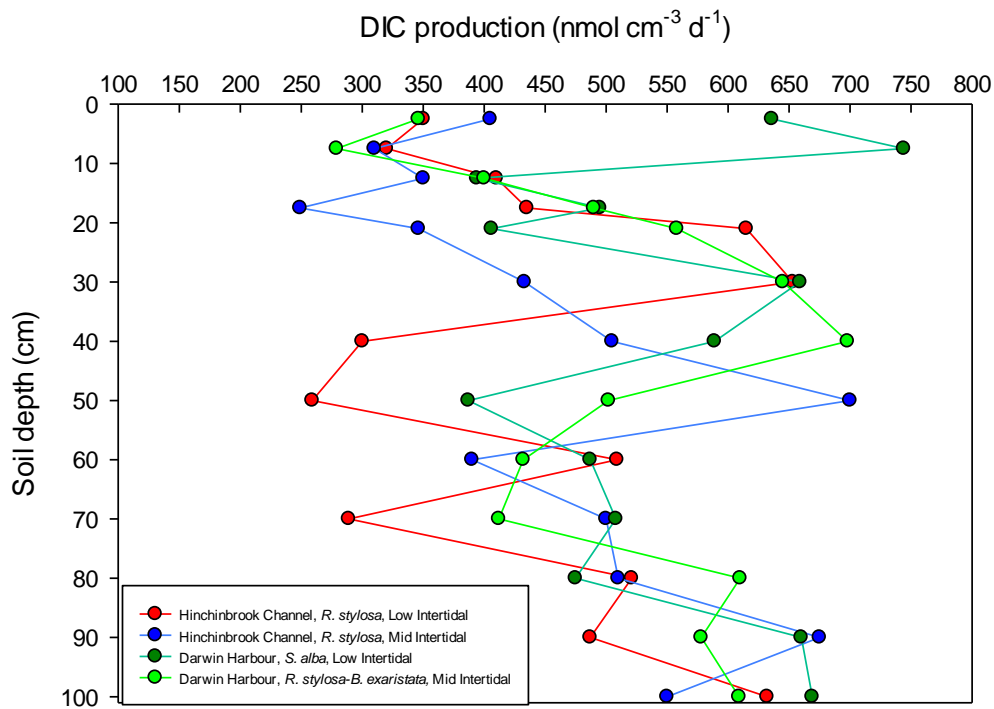


Figure 2. Vertical profiles of mean rates of DIC production at intervals to a soil depth of 1 m. Core samples and sample processing details were identical to the methods described in [54–63]. The mangroves at Hinchinbrook Channel, north Queensland, Australia, were sampled in June 2014, and the Darwin Harbour mangroves in the Northern Territory, Australia, were sampled in October 2014.

2.3. Comparing Surface and Subsurface CO_2 Fluxes

Ten studies to date have simultaneously measured CO_2 fluxes across the soil surface and in subsurface deposits in mangrove forests in Australia, Southeast Asia, China, and East Africa [54–63]. Rates of CO_2 production across the soil-water/air interface averaged $1878.3 \pm 230.0 \text{ mg C m}^{-2} \text{ d}^{-1}$ and rates of subsurface DIC production were nearly three times greater, averaging $5188.0 \pm 630.3 \text{ mg C m}^{-2} \text{ d}^{-1}$. Even assuming inaccuracies from methodological shortcomings, subsurface DIC production is clearly greater than CO_2 production at the soil surface. Nevertheless, there was a positive correlation between both sets of measurements (Figure 3), indicating that mineralization rates in surface and subsurface soils respond to identical factors, such as temperature, salinity, pH, frequency of tidal inundation, forest age and composition, root activities, microbial community composition, and soil nutrient and C_{ORG} content.

The extent of the discrepancy between both sets of measurements increases with increasing topographic height (m above mean sea level), indicating that there is a ‘DIC reservoir-pump system’ [2] beneath the forest floor (Figure 4). The greater the tidal elevation of a forest, the greater the discrepancy between carbon respiration at the soil surface and in deep soils. That is, the volume of soil susceptible to drainage increases with forest height above mean sea level. The cause of this phenomenon is that the deeper soils act like a sponge through which porewater is pumped by tidal advection and/or seeps from the forest floor laterally to adjacent waters. Such drainage has also been observed in tidal marshes [64,65].

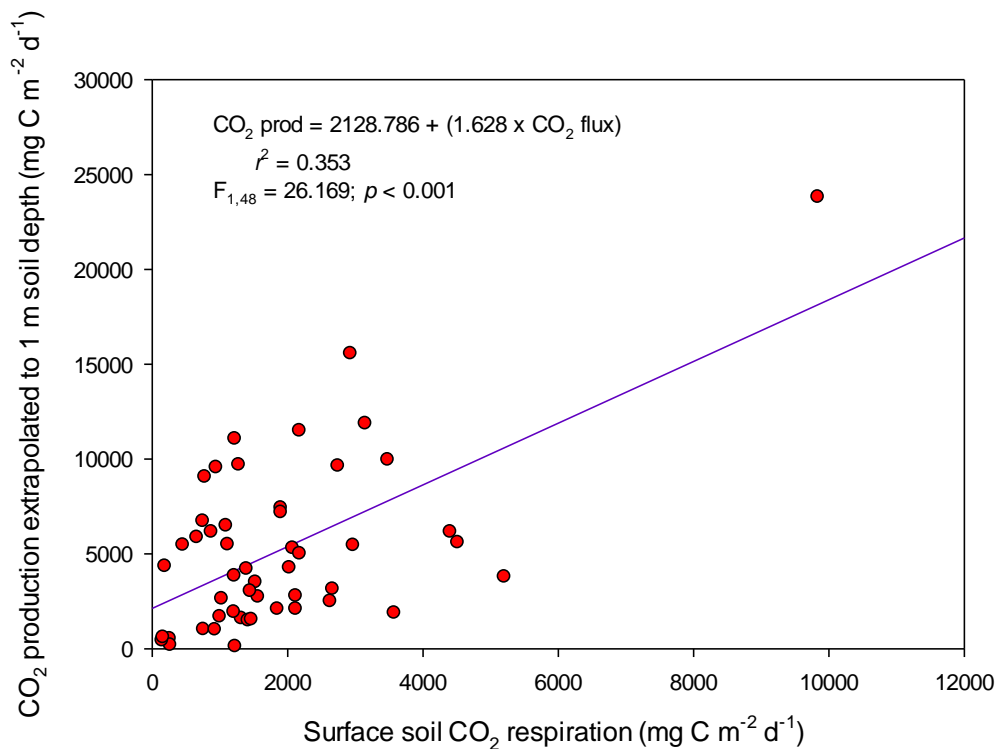


Figure 3. The relationship between surface soil CO₂ respiration and DIC production extrapolated to a soil depth of 1 m (see text for explanation) in mangrove forests across several locations worldwide. The regression equation and coefficient are significant for $n = 50$ total measurements.

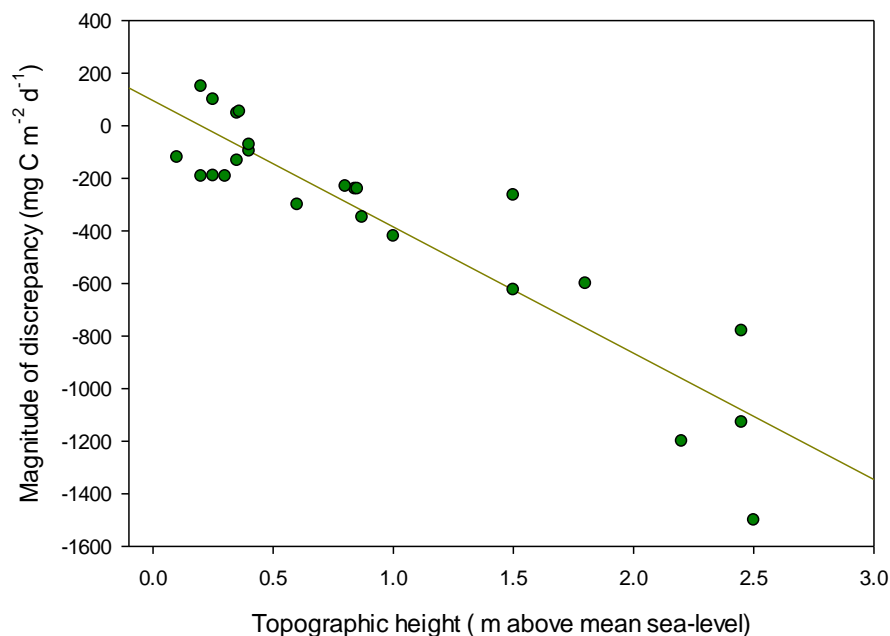


Figure 4. An inverse relationship of increasing discrepancies between surface and subsurface mineralization rates with increasing topographic height in various mangrove forests of Timor-Leste, Thailand, Malaysia, Indonesia, and Australia. Data obtained from references [54–63].

Seepage of groundwater is controlled by complex hydrologic factors [8] that result in porewater oozing out through the bottom soil layers, seen most clearly at low tide as water moving through seepage runnels between the forest and the adjacent creek bank.

3. Composition of Mangrove Tidal Waters

The transport of porewater from the forest floor results in the supersaturation of total alkalinity, $p\text{CO}_2$, free CO_2 , DIC, and CH_4 , and CO_2 outgassing of adjacent mangrove tidal waters (Table 1). Most measurements have been made of $p\text{CO}_2$ and carbon gas fluxes, and vary seasonally and over tidal cycles, but the data are consistent among locations in showing high concentrations that are above saturation thresholds calculated on the basis of salinity and temperature [34,66–93].

Table 1. Mean ($\pm 1\text{SE}$) and median concentrations of alkalinity (μM), $p\text{CO}_2$ (μatm), CO_2 (μM), dissolved inorganic carbon (DIC, μM), and CH_4 (nM) and CO_2 ($\text{mmol m}^{-2} \text{d}^{-1}$) and CH_4 fluxes ($\mu\text{mol m}^{-2} \text{d}^{-1}$) across the water-air interface in mangrove waters worldwide. Data from [66–93].

Parameters	Mean	Median	Number of Measurements
Total alkalinity	1317.6 \pm 153.3	1211.0	41
$p\text{CO}_2$	3202.8 \pm 306.6	1233.0	219
CO_2	1446.3 \pm 162.3	1270.5	44
DIC	1838.0 \pm 71.4	2024.0	83
CH_4	244.7 \pm 49.1	135.5	60
CO_2 fluxes	78.9 \pm 8.0	50.0	143
CH_4 fluxes	530.4 \pm 78.5	260.1	134

4. Estimates of Tidal Export of DIC, DOC, POC, CH_4 , and Alkalinity

High concentrations of DIC, DOC, CH_4 , and total alkalinity in the interstitial water pool and subsurface transport results in significant export to adjacent tidal waters of the coastal ocean (Table 2). Only comparatively few locations, most in Australia, have been used to measure transport, but they are consistent in revealing high rates of export. Mean DIC, alkalinity, DOC, and CH_4 exports were 339.6, 211.5, 229.1, and 0.66 $\text{mmol m}^{-2} \text{d}^{-1}$, respectively (Table 2).

Unlike the data for DIC, alkalinity, and CH_4 , there are earlier estimates of DOC export, as summarized by Adame and Lovelock [7]. Combining the data in Table 2 and in [7], DOC export averaged 85.3 \pm 35.8 ($\pm 1 \text{SE}$) $\text{mmol m}^{-2} \text{d}^{-1}$ over 41 measurements. POC export, derived from data in [7,10], averaged 25.1 \pm 9.2 ($\pm 1 \text{SE}$) $\text{mmol m}^{-2} \text{d}^{-1}$ over 63 measurements.

Table 2. Mean ($\pm 1 \text{SE}$) rates ($\text{mmol m}^{-2} \text{d}^{-1}$) of DIC, total alkalinity, dissolved organic carbon (DOC), and CH_4 export from mangrove forests to adjacent mangrove and coastal waters measured recently from various locations worldwide. These empirical estimates were derived from using a Eulerian approach of time-series water sampling and tracing of radium isotopes. ND = no data.

Location	DIC Export	Alkalinity Export	DOC Export	CH_4 Export	Reference
Southern Moreton Bay, Queensland, Australia	186 \pm 37	69 \pm 14	72 \pm 15	0.014 \pm 0.0023	[94]
	205 \pm 41	88 \pm 18	65 \pm 13	0.0056 \pm 0.0011	
	247 \pm 49	132 \pm 26	40 \pm 8	0.017 \pm 0.0034	
Evans River estuary, New South Wales, Australia	125 \pm 82	51 \pm 34	136 \pm 89	0.6 \pm 0.4	[95]
	559 \pm 292	321 \pm 172	562 \pm 293	2.3 \pm 1.4	
	165 \pm 102	59 \pm 37	202 \pm 125	0.8 \pm 0.6	
	177 \pm 100	67 \pm 39	233 \pm 132	0.9 \pm 0.6	
Maowei Sea, Guangxi Province, south China	700 \pm 820	ND	310 \pm 300	ND	[96]
	250 \pm 240		250 \pm 230		
Eastern Gulf of Carpentaria, Australia	440.4 \pm 232.6	365.5 \pm 177.2	846.1 \pm 936.5	ND	[97]
	146.2 \pm 125.1	896.4 \pm 459.3	176.2 \pm 529.9		
	610.9 \pm 342.0	564.0 \pm 383.5	2110.5 \pm 1762.8		
	774.3 \pm 223.5	726.9 \pm 261.0	294.2 \pm 1276.2		
	730.0 \pm 416.5	679.2 \pm 367.3	153.4 \pm 626.7		

Table 2. Cont.

Location	DIC Export	Alkalinity Export	DOC Export	CH ₄ Export	Reference
Can Gio, Saigon River, southern Vietnam	351.6 ± 33.9		20.6 ± 1.9		[98]
	480.0 ± 35.6		31.0 ± 2.3		
	677.7 ± 79.0	ND	67.7 ± 7.9	ND	
	612.2 ± 71.4		60.0 ± 3.7		
	338.9 ± 39.5		33.3 ± 2.0		
Six mangrove estuaries, north, northeast, and southeast Australia	85	116			[99]
	22	21	7.5 ± 0.2		
	−97	81	3.3 ± 0.4	ND	
	83	12	5.1 ± 0.5		
	77	116	4.2 ± 0.2		
−3	−1				
Badeldaob Island, Palau	79 ± 28	48 ± 17	35 ± 12	ND	[100]
	10 ± 4	2 ± 1	8 ± 3		
Indian Sundarbans	202.3	ND	162.1	ND	[101]
Korogoro Creek, New South Wales, Australia	687	23	294.8	ND	[102]
Harney and Shark Rivers, Florida Everglades	574.5	ND	ND	ND	[103]
	1031.5 ± 291.3				
Mean ± 1SE	339.6 ± 51.5	211.5 ± 58.2	229.1 ± 78	0.66 ± 0.29	

5. Carbon Flow through the World's Mangrove Ecosystems and Contributions to the Coastal Ocean

Until the availability of the empirical data referenced in Tables 1 and 2 indicating supersaturated conditions in adjacent mangrove waters, large subsurface pools of interstitial DIC and DOC implied that large amounts of dissolved carbon might be exported from the forest, possibly accounting for as much as 112–160 Tg a^{−1} of mangrove carbon to balance the budgets constructed by Bouillon et al. [104] (as revised by Beithaupt et al. [105]) and Alongi [2,10]. This discrepancy was called the “missing carbon”. Without empirical data, Alongi [2] estimated DOC and DIC export by difference, resulting in estimates of 15 Tg a^{−1} and 86 Tg a^{−1} for DOC and DIC, respectively.

Here, the mass balance model of carbon flow through the world's mangrove ecosystems constructed by Alongi [2] is revised, using the data in Sections 2.1–2.3 and in Table 2, and newer data for soil + root burial [3,106], root production [107], mangrove gross primary production (GPP), POC, and DOC export [7,10], and canopy respiration (R_c) [19,66,108–114], and extrapolated using the most recent estimate of global mangrove area [115]. The revised carbon flow model (Figure 5) shows that ~64% of GPP is respired by the canopy with NPP vested nearly equally in the litter, wood, and belowground root production. About 41% of litter production is exported to adjacent tidal waters, and as estimated by difference, about 40% is buried and 44% incorporated and eventually decomposed in the massive soil C_{ORG} pool (5396 Tg). C_{ORG} burial (14 Tg C a^{−1}) equates to about 12% of NPP. Of the combined total carbon mineralization (subsurface DIC production + CO₂ respiration at the soil surface), 25% is released at the forest floor surface in a separate process, and approximately all subsurface DIC production is exported to adjacent tidal waters in the form of DOC (~30%), dissolved CH₄ (<0.2%) and DIC (~70%). A considerable, but unquantified, amount of exported DIC, DOC, and CH₄ is derived from groundwater derived from adjacent upland [13,74–76,94–97,101,103], so it is unclear exactly how much dissolved carbon exported from mangroves is derived from soil mineralization.

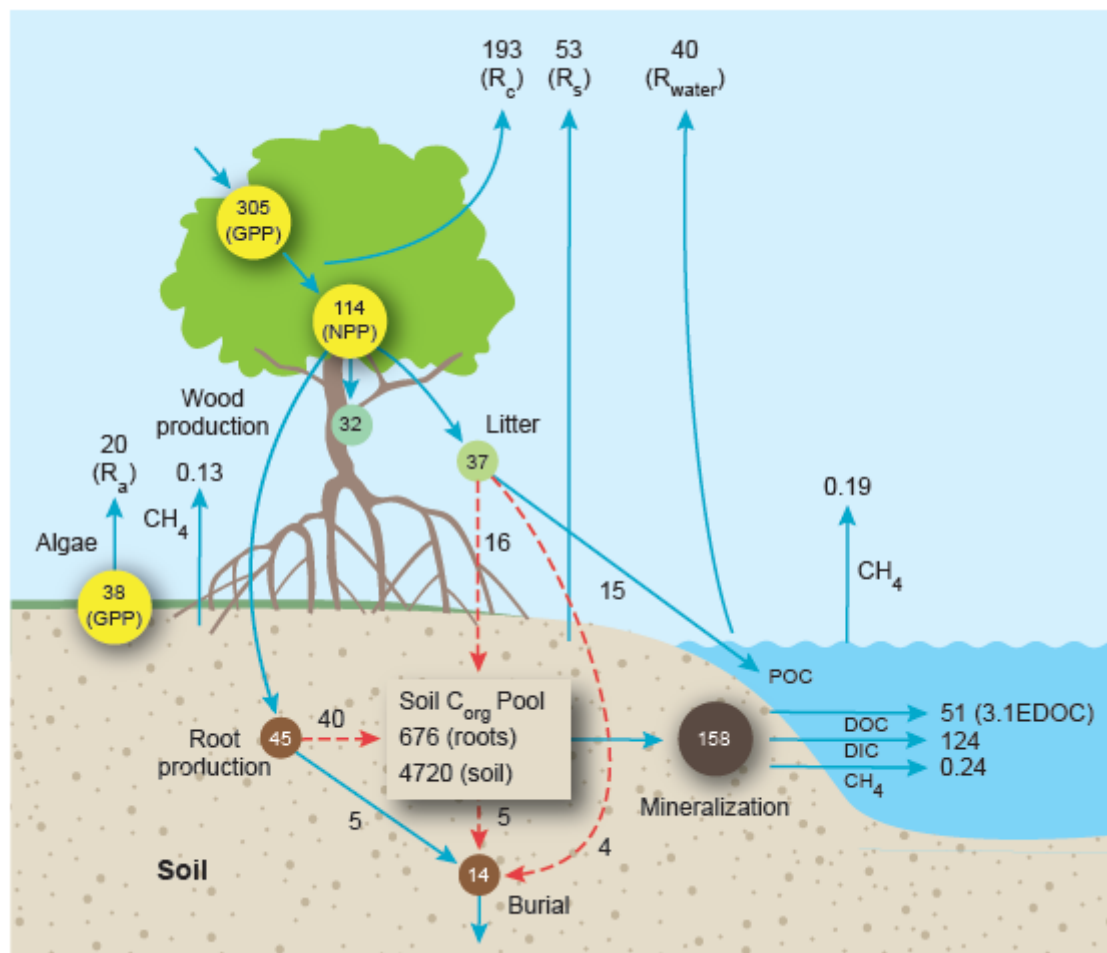


Figure 5. A mass balance model of carbon flow through the world's mangrove ecosystems, updated from [2]. Units are Tg C a^{-1} . The budget assumes a global mangrove area of $86,495 \text{ km}^2$ [116]. Solid blue arrows represent mean values based on empirical data (see text for explanation and references.) Dashed red arrows represent mean values estimated indirectly (by difference). The C_{org} pool (both roots and soil) in soils to a depth of 1 m is presented as a box in the forest floor with units of Tg C . Unquantified inputs of dissolved carbon from land-derived groundwater and organic matter inputs from adjacent marine and catchments are not depicted. Abbreviations: GPP = gross primary production; NPP = net primary production; R_{Aa} = algal respiration; R_{C} = canopy respiration; R_{S} = soil respiration at soil surface; R_{WATER} = waterway respiration; POC = particulate organic matter; DIC = dissolved inorganic carbon; DOC = dissolved organic carbon; CH_4 = methane; EDOC = exchangeable dissolved organic carbon.

The supersaturation of mangrove waters leads to significant CO_2 (40 Tg C a^{-1}) and CH_4 (0.19 Tg C a^{-1}) release to the atmosphere. The rates of soil mineralization imply that the turnover time of the entire soil C_{ORG} pool is on the order of 25 years. This time frame is supported by empirical findings that mangrove roots decompose slowly [106] and that mangrove soil organic matter is composed mostly of allochthonous, highly-refractory, plant-derived material that is high in lignocellulose, and hemicellulose derived mostly from leaves [116] that decompose slowly [117]. About 58% of soil carbon is mangrove-derived, a value that comes from stable isotope signatures of mangrove soils [118], and about one-third of the total soil carbon pool is composed of dead roots [2,10] that also decompose slowly [106]. Assuming that 4 Tg C a^{-1} of litter is buried and that all POC export is derived from litter, then the remaining 16 Tg a^{-1} of litter produced must fall to the forest floor where it is presumably incorporated into detritus food webs and eventually mineralized in situ. Wood that falls to the forest floor may be eventually incorporated into the soil pool, but decomposition is very

slow [119] and likely a minor flux, so it is not included in the mass balance; also not included are benthos and zooplankton production and chemical defenses. The total soil mineralization equates to approximately 140% of mangrove NPP. This anomaly suggests that: (1) inputs from allochthonous marine and terrestrial sources are necessary to balance the mineralization outputs (158 Tg C a^{-1}); (2) a large proportion of the soil pool and its subsequent decomposition is derived from the intertidal mudflat prior to mangrove colonization; (3) wood, algae, and fauna contribute to the soil pool; and/or (4) the subsurface soil mineralization rates and subsequent export data are overestimated. It is also conceivable that root production is underestimated given that the empirical dataset (mostly for estimates of fine roots) is small and that there are some methodological shortcomings in deriving production estimates [10,107].

Analysis of the origin of mangrove soil organic matter indicates that about 42% of the organic matter may be derived from external sources [14,118]. Measurements of radiogenic and stable isotopes in a subtropical Australian mangrove indicate that century-old sequestered carbon is still susceptible to remineralization and tidal export [120], supporting the idea that organic carbon deposited prior to mangrove colonization continues to be decomposed, as all mangroves colonize intertidal mudflats that have considerable amounts of soil C_{ORG} [6]. Mangrove DIC export contributes nearly 60% of DIC, and 27% of DOC discharged from the world's tropical rivers to the coastal ocean, based on comparison with tropical riverine export values in Huang et al. [121]. Mangroves inhabit only 0.3% of global coastal ocean area but contribute 55% of air-sea exchange compared with the global average [122], 28% of DIC export, 14% of C burial, and 13% of DOC + POC export, compared to global averages in [123] for the world's coastal ocean. Mangrove ecosystems thus contribute a disproportionate share to carbon cycling in tropical seas and in the global coastal ocean.

The mass balance model is only a tool to identify the major and minor pathways of carbon flow in mangrove ecosystems and is not meant to be absolute as it does not distinguish known site-specific differences in soil type, forest composition and age, tidal exchange, bioturbation, and rates of forest productivity. As noted in the tables and figures, there are considerable variations in the mean of most measurements that are not represented in the model. Nevertheless, the model is helpful in suggesting where more research is needed, such as in more measurements of canopy GPP and respiration, preferably using the eddy covariance method, root production, estimates of DOC, CH_4 , and especially DIC export, as well as more empirical measurements of subsurface DIC production as well as a clearer understanding of the contribution of groundwater derived from upland and inputs from allochthonous sources, such as the adjacent catchment and coastal zone.

Net ecosystem production (NEP), derived by subtracting all respiratory losses (ecosystem respiration, $R_E = R_C + R_S + R_{\text{WATER}} + R_{\text{MICROALGAE}}$) from all mangrove, algal, and phytoplankton gross primary production (GPP) is $628 \text{ g C m}^{-2} \text{ a}^{-1}$ and 54 Tg C a^{-1} for the world's mangroves. Phytoplankton GPP and R in mangrove tidal creeks and waterways (total area = 7208 km^2 assuming a forest: waterway area ratio of 12 [10]) averaged 1524.4 and $846.9 \text{ mg C m}^{-2} \text{ d}^{-1}$ [10]. Subsurface soil respiration was excluded from the ecosystem respiration estimate because (1) the core incubation method used to measure subsurface respiration is crude and may be an overestimate; (2) it is unclear how much porewater DIC is actually derived from groundwater; and (3) the proportional amounts of dissolved carbon derived from groundwater and from subsurface respiration is unknown.) R_E was $3558 \text{ g C m}^{-2} \text{ a}^{-1}$ for a global R_E of 306 Tg C a^{-1} , and total GPP was $4186 \text{ g C m}^{-2} \text{ a}^{-1}$ for a global GPP of 360 Tg C a^{-1} . The ratio of P_{GPP}/R_E averaged 1.18, indicating that mangrove ecosystems are net autotrophic.

6. Conclusions

The mangrove forest floor is unique, with cracks, fissures, extensive roots, burrows, tubes, and drainage channels, and its dynamic nature facilitates non-steady-state early diagenesis of organic matter in the soil. Rate processes and edaphic conditions (e.g., temperature, redox status, salinity) oscillate in synchrony with tidal flushing and inundation and other factors such as the extent of bioturbation and

weather. Rates of soil C_{ORG} mineralization and belowground C_{ORG} stocks are high, indicating rapid accumulation and recycling of organic matter within the deep (>1 m) soil horizon. On average, carbon respiration across the surface soil-air/water interface equates to only 25% of total carbon mineralized within the entire soil horizon as most respired carbon is released in a dissolved form via advective porewater exchange and/or lateral transport and subsurface tidal pumping to adjacent tidal waters. A revised carbon budget for the world's mangrove ecosystems indicates that subsurface respiration is the second-largest respiratory flux after canopy respiration. The amounts of dissolved carbon released to adjacent tidal waters are sufficient to cause pCO_2 oversaturation of the water column, leading to tropical coastal waters being a source of CO_2 to the atmosphere. Mangrove DIC and DOC discharge contribute disproportionately to dissolved carbon discharge from the world's low latitude rivers to the tropical coastal ocean and contribute 55% of air-sea exchange, 28% of DIC export, 14% of C burial, and 13% of DOC + POC export from the world's wetlands and estuaries to the coastal ocean.

Funding: This research received no external funding.

Conflicts of Interest: The author declares no conflict of interest.

References

1. Donato, D.C.; Kauffman, J.B.; Murdiyarso, D.; Kurnianto, S.; Stidham, M.; Kanninen, M. Mangroves among the most carbon-rich forests in the tropics. *Nat. Geosci.* **2011**, *4*, 293–297. [[CrossRef](#)]
2. Alongi, D.M. Carbon cycling and storage in mangrove forests. *Annu. Rev. Mar. Sci.* **2014**, *6*, 195–219. [[CrossRef](#)] [[PubMed](#)]
3. Alongi, D.M. Global significance of mangrove blue carbon in climate change mitigation. *Science* **2020**, *2*, 57. [[CrossRef](#)]
4. Lovelock, C.E.; Krauss, K.W.; Osland, M.J.; Reef, R.; Ball, M.C. The physiology of mangrove trees with changing climate. In *Tropical Tree Physiology*; Goldstein, G., Santiago, L.S., Eds.; Springer: Cham, Switzerland, 2016; pp. 149–179.
5. Feller, I.C.; Lovelock, C.E.; Berger, U.; McKee, K.L.; Joye, S.B.; Ball, M.C. Biocomplexity in mangrove ecosystems. *Annu. Rev. Mar. Sci.* **2010**, *2*, 395–417. [[CrossRef](#)] [[PubMed](#)]
6. Alongi, D.M. Mangroves. In *Encyclopedia of Estuaries*; Kennish, M., Ed.; Springer: Berlin, Germany, 2016; pp. 393–404.
7. Adame, M.E.; Lovelock, C.E. Carbon and nutrient exchange of mangrove forests with the coastal ocean. *Hydrobiologia* **2011**, *663*, 23–50. [[CrossRef](#)]
8. Mazda, Y.; Wolanski, E.; Ridd, P.V. *The Role of Physical Processes in Mangrove Environments: Manual for the Preservation and Utilization of Mangrove Ecosystems*; Terapub: Tokyo, Japan, 2007.
9. Woodroffe, C.D.; Rogers, K.; McKee, K.L.; Lovelock, C.E.; Mendelssohn, I.A.; Saintilan, N. Mangrove sedimentation and response to relative sea-level rise. *Annu. Rev. Mar. Sci.* **2016**, *8*, 243–266. [[CrossRef](#)]
10. Alongi, D.M. *The Energetics of Mangrove Forests*; Springer: Dordrecht, The Netherlands, 2009.
11. Alongi, D.M.; Mukhopadhyay, S.K. Contribution of mangroves to coastal carbon cycling in low latitude seas. *Agric. For. Meteorol.* **2015**, *213*, 266–272. [[CrossRef](#)]
12. Jennerjahn, T.C.; Ittekkot, V. Relevance of mangroves for the production and deposition of organic matter along tropical continental margins. *Naturwissenschaften* **2002**, *89*, 23–30. [[CrossRef](#)]
13. Maher, D.T.; Call, M.; Santos, I.R.; Sanders, C.J. Beyond burial: Lateral exchange is a significant atmospheric carbon sink in mangrove forests. *Biol. Lett.* **2018**, *14*, 20180200. [[CrossRef](#)]
14. Kristensen, E.; Connolly, R.M.; Otero, X.L.; Marchand, C.; Ferreira, T.O.; Rivera-Monroy, V.H. Biogeochemical cycles: Global approaches and perspectives. In *Mangrove Ecosystems: A Global and Biogeographic Perspectives*; Rivera-Monroy, V.H., Lee, S.Y., Kristensen, E., Twilley, R.R., Eds.; Springer: Cham, Switzerland, 2017; pp. 163–209.
15. Alongi, D.M. Mangrove-microbe-soil relations. In *Interactions between Macro- and Microorganisms in Marine Sediments*; Kristensen, E., Haese, R.R., Kostka, J.K., Eds.; American Geophysical Union: Washington, DC, USA, 2005; pp. 85–103.

16. Hopkinson, C.S.; Smith, E.M. Estuarine respiration: An overview of benthic, pelagic, and whole system respiration. In *Respiration in Aquatic Ecosystems*; del Giorgio, P.A., Williams, P.J.I.B., Eds.; Oxford University Press: Oxford, UK, 2005; pp. 122–146.
17. Castillo, J.A.A.; Apan, A.A.; Maraseni, T.N.; Salmo, S.G., III. Soil greenhouse gas fluxes in tropical mangrove forests and in land uses on deforested mangrove lands. *Catena* **2017**, *159*, 60–69. [[CrossRef](#)]
18. Sea, M.A.; Garcias-Bonet, N.; Saderne, V.; Duarte, C.M. Carbon dioxide and methane emissions from Red Sea mangrove sediments. *Biogeosci. Discuss.* **2018**. [[CrossRef](#)]
19. Rodda, S.R.; Thumaty, K.C.; Jha, C.S.; Dadhwal, V.K. Seasonal variations of carbon dioxide, water vapor and energy fluxes in tropical Indian mangroves. *Forests* **2016**, *7*, 35. [[CrossRef](#)]
20. Cameron, C.; Hutley, L.B.; Friess, D.A.; Brown, B. High greenhouse gas emissions mitigation benefits from mangrove rehabilitation in Sulawesi, Indonesia. *Ecosyst. Serv.* **2019**, *40*, 101035. [[CrossRef](#)]
21. Lovelock, C.E.; Feller, I.C.; Reef, R.; Ruess, R.W. Variable effects of nutrient enrichment on soil respiration in mangrove forests. *Plant Soil* **2014**, *379*, 135–148. [[CrossRef](#)]
22. Middelburg, J.J.; Nieuwenhuize, J.; Slim, F.J.; Ohowa, B. Sediment biogeochemistry in an East African mangrove forest (Gazi Bay, Kenya). *Biogeochemistry* **1996**, *34*, 133–155. [[CrossRef](#)]
23. Alongi, D.M. The role of soft-bottom benthic communities in tropical mangrove and coral reef ecosystems. *Rev. Aquat. Sci.* **1989**, *1*, 243–280.
24. Alongi, D.M. Zonation and seasonality of benthic primary production and community respiration in tropical mangrove forests. *Oecologia* **1994**, *98*, 320–327. [[CrossRef](#)] [[PubMed](#)]
25. Alongi, D.M.; Christoffersen, P.; Tirendi, F. The influence of forest type on microbial-nutrient relationships in tropical mangrove sediments. *J. Exp. Mar. Biol. Ecol.* **1993**, *171*, 201–223. [[CrossRef](#)]
26. Blackburn, T.H.; Christensen, D.; Fanger, A.M.; Henriksen, K.; Iizumi, H.; Ivensen, N.; Limpsaichol, P. Mineralization processes in mangrove and seagrass sediments. In *Ao Yon—A Mangrove in the Andaman Sea*; Hylleberg, J., Ed.; Institute of Ecology and Genetics, University of Aarhus: Aarhus, Denmark, 1987; pp. 22–32.
27. Dye, A.H. Oxygen consumption by sediments in a Southern African mangrove swamp. *Estuar. Coast. Shelf Sci.* **1983**, *17*, 473–478. [[CrossRef](#)]
28. Kristensen, E.; Andersen, F.Ø.; Kofoed, L.H. Preliminary assessment of benthic metabolism in a south-east Asian mangrove swamp. *Mar. Ecol. Prog. Ser.* **1988**, *48*, 137–145. [[CrossRef](#)]
29. Kristensen, E.; Holmer, M.; Bussarawit, N. Benthic metabolism and sulfate reduction in a south-east Asian mangrove swamp. *Mar. Ecol. Prog. Ser.* **1991**, *73*, 93–103. [[CrossRef](#)]
30. Kristensen, E.; Devol, A.H.; Ahmed, S.I.; Saleem, M. Preliminary study of benthic metabolism and sulfate reduction in a mangrove swamp in the Indus delta, Pakistan. *Mar. Ecol. Prog. Ser.* **1992**, *90*, 287–297. [[CrossRef](#)]
31. Kristensen, E.; King, G.M.; Holmer, M.; Banta, G.T.; Jensen, M.H.; Hansen, K.; Bussarawit, N. Sulfate reduction, acetate turnover and carbon metabolism in sediments of Ao Nam Bor mangrove, Phuket, Thailand. *Mar. Ecol. Prog. Ser.* **1994**, *109*, 245–255. [[CrossRef](#)]
32. Nedwell, D.B.; Blackburn, T.H.; Wiebe, W.J. Dynamic nature of the turnover of organic carbon, nitrogen and sulphur in the sediments of a Jamaican mangrove forest. *Mar. Ecol. Prog. Ser.* **1994**, *110*, 223–231. [[CrossRef](#)]
33. Padhy, S.R.; Bhattacharyya, P.; Dash, P.K.; Reddy, C.S.; Chakraborty, A.; Pathak, H. Seasonal fluctuation in the three mode of greenhouse gases emission in relation to soil labile carbon pools in degraded mangrove, Sundarbans, India. *Sci. Total Environ.* **2020**, *705*, 135909. [[CrossRef](#)] [[PubMed](#)]
34. Kristensen, E.; Flindt, M.R.; Ulomi, S.; Borges, A.V.; Abril, G.; Bouillon, S. Emission of CO₂ and CH₄ to the atmosphere by sediments and open waters in two Tanzanian mangrove forests. *Mar. Ecol. Prog. Ser.* **2008**, *370*, 53–67. [[CrossRef](#)]
35. Leopold, A.; Marchand, C.; Deborde, J.; Chaduteau, C.; Allenbach, M. Influence of mangrove zonation on CO₂ fluxes at the sediment-air interface (New Caledonia). *Geoderma* **2013**, *202*, 62–70. [[CrossRef](#)]
36. Ouyang, X.; Lee, S.Y.; Connolly, R.M. Structural equation modelling reveals factors regulating surface sediment organic carbon content and CO₂ efflux in a subtropical mangrove. *Sci. Total Environ.* **2017**, *578*, 513–522. [[CrossRef](#)]
37. Lovelock, C.E. Soil respiration and belowground carbon allocation in mangrove forests. *Ecosystems* **2008**, *11*, 342–354. [[CrossRef](#)]

38. Gillis, L.G.; Belshe, E.F.; Narayan, G.R. Deforested mangroves affect the potential for carbon linkages between connected ecosystems. *Estuar. Coast.* **2017**, *40*, 1207–1213. [[CrossRef](#)]
39. Bulmer, R.H.; Schwendenmann, L.; Lohrer, A.M.; Lundquist, C.J. Sediment carbon and nutrient fluxes from cleared and intact temperate mangrove ecosystems and adjacent sandflats. *Sci. Total Environ.* **2017**, *599*, 1874–1884. [[CrossRef](#)] [[PubMed](#)]
40. Grellier, S.; Janeau, J.-L.; Hoai, N.D.; Kim, C.N.T.; Phuong, Q.L.T.; Thu, T.P.T.; Tran-Thi, N.-T.; Marchand, C. Changes in soil characteristics and C dynamics after mangrove clearing (Vietnam). *Sci. Total Environ.* **2017**, *593–594*, 654–663. [[CrossRef](#)] [[PubMed](#)]
41. Gao, G.-F.; Zhang, X.-M.; Li, P.-F.; Simon, M.; Shen, Z.-J.; Chen, J.; Gao, C.-H.; Zheng, H.-L. Examining soil carbon gas (CO₂, CH₄) emissions and the effect on functional microbial abundances in the Zhangjiang Estuary Mangrove Reserve. *J. Coast. Res.* **2020**, *36*, 54–62. [[CrossRef](#)]
42. Alongi, D.M.; Ramanathan, A.L.; Kannan, L.; Tirendi, F.; Trott, L.A.; Bala Krishna Prasad, M. Influence of human-induced disturbance on benthic microbial metabolism in the Pichavaram mangroves, Vellar-Coleroon complex, India. *Mar. Biol.* **2005**, *147*, 1033–1044. [[CrossRef](#)]
43. Pongpam, S.; Komiyama, A.; Tanaka, A.; Sangtuan, T.; Maknual, C.; Kato, S.; Tanapermpool, P.; Patanaponpaiboon, P. Carbon dioxide emission through soil respiration in a secondary mangrove forest of eastern Thailand. *J. Trop. Ecol.* **2009**, *25*, 393–400. [[CrossRef](#)]
44. Gocke, K.; Vitola, M.; Rojas, G. Oxygen consumption patterns in a mangrove swamp on the Pacific coast of Costa Rica. *Rev. Biol. Trop.* **1981**, *29*, 143–154.
45. Golley, F.B.; Odum, H.T.; Wilson, R.F. The structure and metabolism of a Puerto Rican red mangrove forest in May. *Ecology* **1962**, *43*, 9–19. [[CrossRef](#)]
46. Chen, G.; Chen, B.; Yu, D.; Tam, N.F.Y.; Ye, Y.; Chen, S. Soil greenhouse gas emissions reduce the contribution of mangrove plants to the atmospheric cooling effect. *Environ. Res. Lett.* **2016**, *11*, 124019. [[CrossRef](#)]
47. Chen, S.; Chmura, G.L.; Wang, Y.; Yu, D.; Ou, D.; Chen, B.; Ye, Y.; Chen, G. Benthic microalgae offset the sediment carbon dioxide emission in subtropical mangrove in cold seasons. *Limnol. Oceanogr.* **2019**, *64*, 11116. [[CrossRef](#)]
48. Chen, G.C.; Ulumuddin, Y.I.; Pramudji, S.; Chen, S.Y.; Chen, B.; Ye, Y.; Ou, D.Y.; Ma, Z.Y.; Huang, H.; Wang, J.K. Rich soil carbon and nitrogen but low atmospheric greenhouse gas fluxes from North Sulawesi mangrove swamps in Indonesia. *Sci. Total Environ.* **2014**, *487*, 91–96. [[CrossRef](#)]
49. Holmer, M.; Andersen, F.Ø.; Kristensen, E.; Thongtham, N. Transformation in the Bangrong mangrove forest-seagrass bed system, Thailand: Seasonal and spatial variations in benthic metabolism and sulfur biogeochemistry. *Aquat. Microb. Ecol.* **1999**, *20*, 203–212. [[CrossRef](#)]
50. Alongi, D.M.; Sasekumar, A.; Tirendi, F.; Dixon, P. The influence of stand age on benthic decomposition and recycling of organic matter in managed mangrove forests in Malaysia. *J. Exp. Mar. Biol. Ecol.* **1998**, *225*, 197–218. [[CrossRef](#)]
51. Lovelock, C.E.; Ruess, R.W.; Feller, I.C. CO₂ efflux from cleared mangrove peat. *PLoS ONE* **2011**, *6*, e21279. [[CrossRef](#)] [[PubMed](#)]
52. Ray, R.; Chowdhury, C.; Majumder, N.; Dutta, M.K.; Mukhopadhyay, S.K.; Jana, T.K. Improved model calculation of atmospheric CO₂ increment in affecting carbon stock of tropical mangrove forest. *Tellus B Chem. Phys. Meteorol.* **2013**, *65*, 18981. [[CrossRef](#)]
53. Kristensen, E.; Mangion, P.; Tang, M.; Flindt, M.R.; Holmer, M.; Ulomi, S. Microbial carbon oxidation and pathways in sediments in two Tanzanian mangrove forests. *Biogeochemistry* **2011**, *103*, 143–158. [[CrossRef](#)]
54. Alongi, D.M.; de Carvalho, N.A.; Amaral, A.L.; da Costa, A.; Trott, L.A.; Tirendi, F. Uncoupled surface and below-ground soil respiration in mangroves: Implications for estimates of dissolved inorganic carbon export. *Biogeochemistry* **2012**, *109*, 151–162. [[CrossRef](#)]
55. Kristensen, E.; Andersen, F.Ø.; Holmboe, N.; Holmer, M.; Thongtham, N. Carbon and nitrogen mineralization in sediments of the Bangrong mangrove area, Phuket, Thailand. *Aquat. Microb. Ecol.* **2000**, *22*, 199–213. [[CrossRef](#)]
56. Alongi, D.M.; Sasekumar, A.; Chong, V.C.; Pfitzner, J.; Trott, L.A.; Dixon, P.; Brunskill, G.J. Sediment accumulation and organic material flux in a managed mangrove ecosystem: Estimates of land-ocean-atmosphere exchange in peninsular Malaysia. *Mar. Geol.* **2004**, *208*, 383–402. [[CrossRef](#)]

57. Alongi, D.M.; Pfitzner, J.; Trott, L.A.; Tirendi, F.; Dixon, P.; Klumpp, D.W. Rapid sediment accumulation and microbial mineralization in forests of the mangrove *Kandelia candel* in the Jiulongjiang estuary, China. *Estuar. Coast. Shelf Sci.* **2005**, *63*, 605–618. [[CrossRef](#)]
58. Alongi, D.M. Carbon dynamics in Southeast Asian mangroves. (Unpublished work).
59. Alongi, D.M.; Trott, L.A.; Rachmansyah, R.; Tirendi, F.; McKinnon, A.D.; Undu, M.C. Growth and development of mangrove forests overlying smothered coral reefs, Sulawesi and Sumatra, Indonesia. *Mar. Ecol. Prog. Ser.* **2008**, *370*, 97–109. [[CrossRef](#)]
60. Alongi, D.M.; Tirendi, F.; Dixon, P.; Trott, L.A.; Brunskill, G.J. Mineralization of organic matter in intertidal sediments of a tropical semi-enclosed delta. *Estuar. Coast. Shelf Sci.* **1999**, *48*, 451–467. [[CrossRef](#)]
61. Alongi, D.M.; Tirendi, F.; Clough, B.F. Below-ground decomposition of organic matter in forests of the mangroves *Rhizophora stylosa* and *Avicennia marina* along the arid coast of Western Australia. *Aquat. Bot.* **2000**, *68*, 97–122. [[CrossRef](#)]
62. Alongi, D.M.; Tirendi, F.; Trott, L.A.; Xuan, T.T. Benthic decomposition rates and pathways in plantations of the mangrove *Rhizophora apiculata* in the Mekong delta, Vietnam. *Mar. Ecol. Prog. Ser.* **2000**, *194*, 87–101. [[CrossRef](#)]
63. Alongi, D.M.; Wattayakorn, G.; Pfitzner, J.; Tirendi, F.; Zagorskis, I.; Brunskill, G.J.; Davidson, A.; Clough, B.F. Organic carbon accumulation and metabolic pathways in sediments of mangrove forests in southern Thailand. *Mar. Geol.* **2001**, *179*, 85–103. [[CrossRef](#)]
64. Chu, S.N.; Wang, Z.A.; Gonneea, M.E.; Kroeger, K.D.; Ganju, N.K. Deciphering the dynamics of inorganic carbon export from intertidal salt marshes using high-frequency measurements. *Mar. Chem.* **2018**, *206*, 7–18. [[CrossRef](#)]
65. Tobias, C.; Neubauer, S.C. Salt marsh biogeochemistry—An overview. In *Coastal Wetlands*; Perillo, G.M.E., Wolanski, E., Cahoon, D.R., Hopkinson, C.S., Eds.; Elsevier: Amsterdam, The Netherlands, 2019; pp. 539–596.
66. Troxler, T.G.; Barr, J.G.; Fuentes, J.D.; Engel, V.; Anderson, G.; Sanchez, C.; Lagomasino, D.; Price, R.; Davis, S.E. Component-specific dynamics of riverine mangrove CO₂ efflux in the Florida Everglades. *Agric. For. Meteorol.* **2015**, *213*, 273–282. [[CrossRef](#)]
67. Ralison, O.H.; Borges, A.V.; Dehairs, F.; Middelburg, J.J.; Bouillon, S. Carbon biogeochemistry of the Betsiboka estuary (north-western Madagascar). *Org. Geochem.* **2008**, *39*, 1649–1658. [[CrossRef](#)]
68. Miyajima, T.; Tsuboi, Y.; Tanaka, Y.; Koike, I. Export of inorganic carbon from two Southeast Asian mangrove forests to adjacent estuaries as estimated by the stable isotope composition of dissolved inorganic carbon. *J. Geophys. Res.* **2009**, *114*, G01024. [[CrossRef](#)]
69. Rosentreter, J.A.; Maher, D.T.; Erler, D.V.; Murray, R.; Eyre, B.D. Seasonal and temporal CO₂ dynamics in three tropical mangrove creeks—A revision of global CO₂ emissions. *Geochim. Cosmochim. Acta* **2018**, *222*, 729–745. [[CrossRef](#)]
70. Call, M.; Santos, I.R.; Dittmar, T.; de Rezende, C.E.; Asp, N.E.; Maher, D.T. High pore-water derived CO₂ and CH₄ emissions from a macro-tidal mangrove creek in the Amazon region. *Geochim. Cosmochim. Acta* **2019**, *247*, 106–120. [[CrossRef](#)]
71. Macklin, P.A.; Suryaputra, I.G.N.A.; Maher, D.T.; Murdiyarso, D.; Santos, I.R. Drivers of CO₂ along a mangrove-seagrass transect in a tropical bay: Delayed groundwater seepage and seagrass uptake. *Cont. Shelf Res.* **2019**, *172*, 57–67. [[CrossRef](#)]
72. Ho, D.T.; Ferrón, S.; Engel, V.C.; Larsen, L.G.; Barr, J.G. Air-water gas exchange and CO₂ flux in a mangrove-dominated estuary. *Geophys. Res. Lett.* **2014**, *41*, 108–113. [[CrossRef](#)]
73. Koné, Y.J.-M.; Borges, A.V. Dissolved inorganic carbon dynamics in the waters surrounding forested mangroves of the Ca Mau Province (Vietnam). *Estuar. Coast. Shelf Sci.* **2008**, *77*, 409–421. [[CrossRef](#)]
74. Maher, D.T.; Cowley, K.; Santos, I.R.; Macklin, P.; Eyre, B.D. Methane and carbon dioxide dynamics in a subtropical estuary over a diel cycle: Insights from automated in situ radioactive and stable isotope measurements. *Mar. Chem.* **2015**, *168*, 69–79. [[CrossRef](#)]
75. Taillardat, P.; Ziegler, A.D.; Friess, D.A.; Widory, D.R.; Van Vinh, T.; David, F.; Nguyễn, T.-N.; Marchand, C. Carbon dynamics and inconstant porewater input in a mangrove tidal creek over contrasting seasons and tidal amplitudes. *Geochim. Cosmochim. Acta* **2018**, *237*, 32–48. [[CrossRef](#)]
76. Atkins, M.L.; Santos, I.R.; Ruiz-Halpern, S.; Maher, D.T. Carbon dioxide dynamics driven by groundwater discharge in a coastal floodplain creek. *J. Hydrol.* **2013**, *493*, 30–42. [[CrossRef](#)]

77. David, F.; Meziane, T.; Tran-Thi, N.-T.; Van, V.T.; Thanh-Nho, N.; Taillardat, P.; Marchand, C. Carbon biogeochemistry and CO₂ emissions in a human impacted and mangrove dominated tropical estuary (Can Gio, Vietnam). *Biogeochemistry* **2018**, *138*, 261–275. [[CrossRef](#)]
78. Bartlett, D.S.; Bartlett, K.B.; Hartman, J.M.; Harriss, R.C.; Sebacher, D.I.; Pelletier-Travis, R.; Dow, D.D.; Brannon, D.P. Methane emissions from the Florida Everglades: Patterns of variability in a regional wetland ecosystem. *Glob. Biogeochem. Cycles* **1989**, *3*, 363–374. [[CrossRef](#)]
79. Dutta, M.K.; Kumar, S.; Mukherjee, R.; Sharma, N.; Acharya, A.; Sanyal, P.; Bhusan, R.; Mukhopadhyay, S.K. Diurnal carbon dynamics in a mangrove-dominated tropical estuary (Sundarbans, India). *Estuar. Coast. Shelf Sci.* **2019**, *229*, 106426. [[CrossRef](#)]
80. Borges, A.V.; Djenidi, S.; Lacroix, G.; Théate, J.; Delille, B.; Frankignoulle, M. Atmospheric CO₂ flux from mangrove surrounding waters. *Geophys. Res. Lett.* **2003**, *30*, 1558. [[CrossRef](#)]
81. Ghosh, S.; Jana, T.K.; Singh, B.N.; Choudhury, A. Comparative study of carbon dioxide system in virgin and reclaimed mangrove waters of Sundarbans during freshnet. *Mahasagar. Bull. Nat. Instit. Oceanogr.* **1987**, *20*, 155–161.
82. Ovale, A.R.C.; Rezende, C.E.; Lacerda, L.D.; Silva, C.A.R. Factors affecting the hydrochemistry of a mangrove creek, Sepetiba Bay, Brazil. *Estuar. Coast. Shelf Sci.* **1990**, *31*, 639–650. [[CrossRef](#)]
83. Bouillon, S.; Frankignoulle, M.; Dehairs, F.; Velimirov, B.; Eiler, A.; Abril, G.; Etcheber, H.; Borges, A.V. Inorganic and organic carbon biogeochemistry in the Gautami Godavari estuary (Andhra Pradesh, India) during pre-monsoon: The local impact of extensive mangrove forests. *Glob. Biogeochem. Cycles* **2003**, *17*, 1114. [[CrossRef](#)]
84. Call, M.; Maher, D.T.; Santos, I.R.; Ruiz-Halpern, S.; Mangion, P.; Sanders, C.J.; Erler, D.V.; Oakes, J.M.; Rosentreter, R.; Eyre, B.D. Spatial and temporal variability of carbon dioxide and methane fluxes over semi-diurnal and spring-neap-spring timescales in a mangrove creek. *Geochim. Cosmochim. Acta* **2015**, *150*, 211–225. [[CrossRef](#)]
85. Biswas, H.; Mukhopadhyay, S.K.; De, T.K. Biogenic controls in the air-water carbon dioxide exchange in the Sundarbans mangrove environment, northeast coast of Bay of Bengal, India. *Limnol. Oceanogr.* **2004**, *49*, 95–101. [[CrossRef](#)]
86. Biswas, H.; Mukhopadhyay, S.K.; Jana, T.K. Spatial and temporal patterns of methane dynamics in the tropical mangrove dominated estuary, NE coast of Bay of Bengal, India. *J. Mar. Syst.* **2007**, *68*, 55–64. [[CrossRef](#)]
87. Bouillon, S.; Middelburg, J.J.; Dehairs, F.; Borges, A.V.; Abril, G.; Flindt, M.R.; Ulomi, S.; Kristensen, E. Importance of intertidal sediment processes and porewater exchange on the water column biogeochemistry in a pristine mangrove creek (Ras Dege, Tanzania). *Biogeosciences* **2007**, *4*, 311–322. [[CrossRef](#)]
88. Bouillon, S.; Dehairs, F.; Velimirov, B.; Abril, G.; Borges, A.V. Dynamics of organic and inorganic carbon across contiguous mangrove and seagrass systems (Gazi Bay, Kenya). *J. Geophys. Res. Biogeosci.* **2007**, *112*, G02018. [[CrossRef](#)]
89. Linto, N.; Barnes, J.; Ramachandran, R.; Divia, J.; Ramachandran, P.; Upstill-Goddard, R.C. Carbon dioxide and methane emissions from mangrove-associated waters of the Andaman Islands, Bay of Bengal. *Estuar. Coast.* **2014**, *37*, 381–398. [[CrossRef](#)]
90. Millero, F.J.; Hiscock, W.T.; Huang, F.; Roche, M.; Zhang, J.Z. Seasonal variation of the carbonate system in Florida Bay. *Bull. Mar. Sci.* **2001**, *68*, 101–123.
91. Ramesh, R.; Purvaja, R.; Neetha, V.; Divia, J.; Barnes, J.; Upstill-Goddard, R.C. CO₂ and CH₄ emissions from Indian mangroves and its surrounding waters. In *Greenhouse Gas and Carbon Balances in Mangrove Coastal Ecosystems*; Tateda, Y., Upstill-Goddard, R.C., Goreau, T., Alongi, D.M., Kristensen, E., Wattayakorn, G., Eds.; Gendai Toshoh: Kanagawa, Japan, 2007; pp. 139–151.
92. Borges, A.V.; Abril, G.; Bouillon, S. Carbon dynamics and CO₂ and CH₄ outgassing in the Mekong delta. *Biogeosciences* **2018**, *15*, 1093–1114. [[CrossRef](#)]
93. Zablocki, J.A.; Andersson, A.J.; Bates, N.R. Diel aquatic CO₂ system dynamics of a Bermudian mangrove environment. *Aquat. Geochem.* **2011**, *11*, 841. [[CrossRef](#)]
94. Maher, D.T.; Santos, I.R.; Golsby-Smith, L.; Gleeson, J.; Eyre, B.D. Groundwater-derived dissolved inorganic and organic carbon exports from a mangrove tidal creek: The missing carbon sink? *Limnol. Oceanogr.* **2013**, *58*, 475–488. [[CrossRef](#)]

95. Santos, I.R.; Maher, D.T.; Larkin, R.; Webb, J.R.; Sanders, C.J. Carbon outwelling and outgassing vs. burial in an estuarine tidal creek surrounded by mangrove and saltmarsh wetlands. *Limnol. Oceanogr.* **2019**, *64*, 996–1013. [[CrossRef](#)]
96. Chen, X.; Zhang, F.; Lao, Y.; Wang, X.; Du, J.; Santos, I.R. Submarine groundwater discharge-derived carbon fluxes in mangroves: An important component of blue carbon budgets? *J. Geophys. Res. Ocean.* **2018**, *123*, 6962–6979. [[CrossRef](#)]
97. Sippo, J.Z.; Maher, D.T.; Schult, K.G.; Sanders, C.J.; McMahon, A.; Tucker, J.; Santos, I.R. Carbon outwelling across the shelf following a massive mangrove dieback in Australia: Insights from radium isotopes. *Geochim. Cosmochim. Acta* **2019**, *253*, 142–158. [[CrossRef](#)]
98. Taillardat, P.; Willemsen, P.; Marchand, C.; Friess, D.A.; Widory, D.; Baudron, P.; Truong, V.V.; Nguyễn, T.-N.; Ziegler, A.D. Assessing the contribution of porewater discharge in carbon export and CO₂ evasion in a mangrove tidal creek (Can Gio, Vietnam). *J. Hydrol.* **2018**, *563*, 303–318. [[CrossRef](#)]
99. Sippo, J.Z.; Maher, D.T.; Tait, D.R.; Holloway, C.; Santos, I.R. Are mangroves drivers or buffers of coastal acidification? Insights from alkalinity and dissolved inorganic carbon export estimates across a latitudinal gradient. *Glob. Biogeochem. Cycles* **2016**, *30*, 753–766. [[CrossRef](#)]
100. Call, M.; Sanders, C.J.; Macklin, P.A.; Santos, I.R.; Maher, D.T. Carbon outwelling and emissions from two contrasting mangrove creeks during the monsoon storm season in Palau, Micronesia. *Estuar. Coast. Shelf Sci.* **2019**, *218*, 340–348. [[CrossRef](#)]
101. Ray, R.; Bsum, A.; Rixen, T.; Gleixner, G.; Jana, T.K. Exportation of dissolved (inorganic and organic) and particulate carbon from mangroves and its implication to the carbon budget in the Indian Sundarbans. *Sci. Total Environ.* **2018**, *621*, 535–547. [[CrossRef](#)]
102. Sadat-Noori, M.; Maher, D.T.; Santos, I.R. Groundwater discharge as a source of dissolved carbon and greenhouse gases in a subtropical estuary. *Estuar. Coast.* **2016**, *39*, 639–656. [[CrossRef](#)]
103. Ho, D.T.; Ferrón, S.; Engel, V.C.; Anderson, W.T.; Swart, P.K.; Price, R.M.; Barbero, L. Dissolved carbon biogeochemistry and export in mangrove-dominated rivers of the Florida Everglades. *Biogeosciences* **2017**, *14*, 2543–2559. [[CrossRef](#)]
104. Bouillon, S.; Borges, A.V.; Castañeda-Moya, E.; Diele, K.; Dittmat, T.; Duke, N.C.; Kristensen, E.; Lee, S.Y.; Marchand, C.; Middelburg, J.J.; et al. Mangrove production and carbon sinks: A revision of global budget estimates. *Glob. Biogeochem. Cycles* **2008**, *22*, GB2013. [[CrossRef](#)]
105. Beithaupt, J.L.; Smoak, J.M.; Smith, T.J., III; Sanders, C.J.; Hoare, A. Organic carbon burial rates in mangrove sediments: Strengthening the global budget. *Glob. Biogeochem. Cycles* **2012**, *26*, GB3011. [[CrossRef](#)]
106. Ouyang, X.; Lee, S.Y.; Connolly, R.M. The role of root decomposition in global mangrove and saltmarsh carbon budgets. *Earth-Sci. Rev.* **2017**, *166*, 53–63. [[CrossRef](#)]
107. Twilley, R.R.; Castañeda-Moya, E.; Rivera-Monroy, V.H.; Rovai, A. Productivity and carbon dynamics in mangrove wetlands. In *Mangrove Ecosystems: A Global and Biogeographic Perspectives*; Rivera-Monroy, V.H., Lee, S.Y., Kristensen, E., Twilley, R.R., Eds.; Springer: Cham, Switzerland, 2017; pp. 113–162.
108. Barr, J.G.; Engel, V.; Fuentes, J.D.; Fuller, D.O.; Kwon, H. Modeling light-use efficiency in a subtropical mangrove forest equipped with CO₂ eddy covariance. *Biogeosciences* **2013**, *10*, 2145–2158. [[CrossRef](#)]
109. Chen, H.; Lu, W.; Yan, G.; Yang, S.; Lin, G. Typhoons exert significant but differential impacts on net ecosystem carbon exchange of subtropical mangrove forests in China. *Biogeosciences* **2014**, *11*, 5323–5333. [[CrossRef](#)]
110. Lovelock, C.E.; Simpson, L.T.; Duckett, L.J.; Feller, I.C. Carbon budgets for Caribbean mangrove forests of varying structure and with phosphorus enrichment. *Forests* **2015**, *6*, 3528–3546. [[CrossRef](#)]
111. Umayangani, M.A.D.; Perera, K.A.R.S. Contribution of vegetation structure on carbon assimilation capacity of mangrove ecosystem: A case study from Negombo estuary, Sri Lanka. *Int. J. Mar. Sci.* **2017**, *7*, 439–446. [[CrossRef](#)]
112. Cui, X.; Liang, J.; Lu, W.; Chen, H.; Liu, F.; Lin, G.; Xu, F.; Luo, Y.; Lin, G. Stronger ecosystem carbon sequestration potential of mangrove wetlands with respect to terrestrial forests in subtropical China. *Agric. For. Meteorol.* **2018**, *249*, 71–80. [[CrossRef](#)]
113. Zhu, X.; Song, L.; Weng, Q.; Huang, G. Linking in situ photochemical reflectance index measurements with mangrove carbon dynamics in a subtropical coastal wetland. *J. Geophys. Res. Biogeosci.* **2019**, *124*. [[CrossRef](#)]
114. Gnanamoorthy, P.; Selvam, V.; Burman, P.K.D.; Chakraborty, S.; Karipot, A.; Nagarajan, R.; Ramasubramanian, R.; Song, Q.; Zhang, Y.; Grace, J. Seasonal variations of net ecosystem (CO₂) exchange in the Indian tropical mangrove forest of Pichavaram. *Estuar. Coast. Shelf Sci.* **2020**, *243*, 106828. [[CrossRef](#)]

115. Hamilton, S.E.; Casey, D. Creation of a high spatio-temporal resolution global database of continuous mangrove forest cover for the 21st century. *Glob. Ecol. Biogeogr.* **2016**, *25*, 729–738. [[CrossRef](#)]
116. Marchand, C.; Lallier-Vergès, E.; Disnar, J.R.; Kéravis, D. Organic carbon sources and transformations in mangrove sediments: A Rock-Eval pyrolysis approach. *Org. Geochem.* **2008**, *39*, 408–421. [[CrossRef](#)]
117. Marchand, C.; Marchand, J.; Disnar, J.R.; Lallier-Vergès, E.; Lottier, N. Early diagenesis of carbohydrates and lignin in mangrove sediments subject to variable redox conditions (French Guiana). *Geochim. Cosmochim. Acta* **2005**, *69*, 131–142. [[CrossRef](#)]
118. Kristensen, E.; Bouillon, S.; Dittmar, T.; Marchand, C. Organic carbon dynamics in mangrove ecosystems: A review. *Aquat. Bot.* **2008**, *89*, 201–219. [[CrossRef](#)]
119. Robertson, A.I.; Daniel, P.A. Decomposition and the annual flux of detritus from fallen timber in tropical mangrove forests. *Limnol. Oceanogr.* **1989**, *34*, 640–646. [[CrossRef](#)]
120. Maher, D.T.; Santos, I.R.; Schulz, K.G.; Call, M.; Jacobsen, G.E.; Sanders, C.J. Blue carbon oxidation revealed by radiogenic and stable isotopes in a mangrove system. *Geophys. Res. Lett.* **2017**, *44*, 4889–4896. [[CrossRef](#)]
121. Huang, T.-H.; Fu, Y.-H.; Pan, P.Y.; Chen, C.-T.A. Fluvial carbon fluxes in tropical rivers. *Curr. Opin. Environ. Sustain.* **2012**, *4*, 162–169. [[CrossRef](#)]
122. Chen, C.-T.A.; Huang, T.-H.; Chen, Y.-C.; Bai, Y.; He, X.; Kang, Y. Air-sea exchanges of CO₂ in the world's coastal seas. *Biogeosciences* **2013**, *10*, 6509–6544. [[CrossRef](#)]
123. Bauer, J.E.; Cai, W.-J.; Raymond, P.A.; Bianchi, T.S.; Hopkinson, C.S.; Regnier, P.A.G. The changing carbon cycle of the coastal ocean. *Nature* **2013**, *504*, 61–70. [[CrossRef](#)] [[PubMed](#)]



© 2020 by the author. Licensee MDPI, Basel, Switzerland. This article is an open access article distributed under the terms and conditions of the Creative Commons Attribution (CC BY) license (<http://creativecommons.org/licenses/by/4.0/>).